Available online at www.sciencedirect.com
SCIENCE DIRECT®
Journal of Chromatography A, 1069 (2005) 99–106
JOURNAL OF CHROMATOGRAPHY A
www.elsevier.com/locate/chroma

Optimization of monoclonal antibody purification by ion-exchange chromatography☆ Application of simple methods with linear gradient elution experimental data

Takashi Ishihara[a,*], Shuichi Yamamoto[b]

[a] *Kirin Brewery Co. Ltd., Takasaki, Gunma 370-0013, Japan*
[b] *Department of Chemical Engineering, Yamaguchi University Tokiwadai, Ube 755-8611, Japan*

Available online 11 November 2004

Abstract

Simple methods for the optimization of ion-exchange chromatography of proteins in our previous papers were applied to cation-exchange chromatography purification of monoclonal antibodies (Mab). We carried out linear gradient elution experiments, and obtained the data for the peak salt concentration and the peak width. From these data, the distribution coefficient as a function of salt concentration, and the height equivalent to a theoretical plate (HETP) as a function of mobile phase velocity were calculated. The optimized linear gradient elution conditions were determined based on the relationship between buffer consumption and separation time. The optimal stepwise elution conditions were determined based on the relationship between the distribution coefficient and the salt concentration.

Keywords: Antibodies; Cation-exchange chromatography; Ion-exchange chromatography; Protein separation; Chromatography models

1. Introduction

Ion-exchange chromatography (IEC) is a major unit operation in protein drug purification processes [1–5]. Both cation- and anion-exchange chromatography steps are generally involved in monoclonal antibody (Mab) purification processes [5]. However, in designing such processes many parameters must be considered such as mobile phase (pH, salt concentration, etc.), stationary phase (type of ion-exchange group, ion-exchange capacity, particle diameter, pore structure, pore size distribution, base matrix property, etc.), column parameters (length, diameter, etc.) and operating variables (flow rate, gradient slope, sample loading, etc.). Therefore, optimization of IEC is labor-intensive and time-consuming.

For example, in linear gradient elution IEC the gradient slope and the flow rate as well as the column length affect the separation behavior in a complicated way [3]. So if the process is not well understood, it is not easy to choose the right conditions, which provide the required resolution, the allowable process time and the desired buffer consumption. Another typical elution method, stepwise (or step gradient) elution IEC, is commonly employed for process IEC. In this elution method, the concentration of the elution buffer is the key variable, which is usually determined by a trial-and-error approach. In addition, the sensitivity of the elution buffer compositions to the separation behavior must be carefully considered [6].

Therefore, rapid and effective optimizing methodologies for the purification process are much expected in process development. Various chromatography models incorporating economics have been developed, and explained in detail by Guiochon and co-workers [4,7].

In this study, we optimized cation-exchange chromatography processes for recombinant Mab purification by using

☆ Presented at the 17th International Symposium on Preparative/Process Chromatography, Baltimore, MD, USA.

* Corresponding author. Tel.: +81 27 353 7385; fax: +81 27 353 7400.
E-mail address: t-ishihara@kirin.co.jp (T. Ishihara).

0021-9673/$ – see front matter © 2004 Elsevier B.V. All rights reserved.
doi:10.1016/j.chroma.2004.10.040

simple methods developed in our previous papers [3,8]. Linear gradient elution experiments were carried out in order to obtain the data on the peak salt concentration and the peak width as a function of gradient slope and/or the flow velocity. Based on the information thus obtained, linear gradient elution and stepwise elution were optimized. The peak shape, the recovery and the purity of the optimized peaks were examined in order to verify the proposed method.

2. Experimental

2.1. Chromatography media and column

HiTrap SP Sepharose FF column (6% cross-linked agarose, sulfopropyl group, particle diameter ca. 100 μm, column size 25 mm × 7.0 mm i.d., total bed volume V_t = 0.96 mL, Amersham Biosciences, Uppsala, Sweden) was used as a cation-exchange chromatography column and media.

2.2. Materials

The model recombinant human monoclonal antibodies Mab A [IgG_1, VH1, Vκ4, isoelectric point (p*I*) ca. 8, M_r ca. 150 000] and Mab B (IgG_1, VH3, Vκ1, p*I* ca. 8, M_r ca. 150 000) used in this study were produced at Kirin (Takasaki, Japan). Other reagents used in these studies were of analytical grade.

2.3. Chromatography apparatus

Most experiments were performed on a fully automated liquid chromatography system ÄKTA explorer 100 (Amersham Biosciences).

2.4. Linear gradient elution experiment

The SP Sepharose FF column was equilibrated with a starting buffer (buffer A: 20 mM sodium phosphate pH 7.0). The Mab sample loading was fixed as 1-mg/mL gel bed. Elution was performed with the final elution buffer (buffer B: 20 mM sodium phosphate pH 7.0 containing 0.5 M NaCl). The linear gradient elution was performed by changing the buffer composition linearly from buffer A to buffer B with time. Namely, the NaCl concentration was increased with time at a fixed pH and buffer compositions. The gradient slopes g (M/mL) were chosen so that gradient volume was 10, 20, 30, or 40 column bed volume. The volumetric flow rate F was 0.5, 1.0, 1.5, or 2.0 mL/min. The linear mobile phase velocity u was calculated with the cross-sectional area A_c and the column bed void fraction ε as $u = F/(A_c\varepsilon)$. The column bed void fraction ε was determined from the peak retention volume of Dextran T 2000 pulses. The experiments were performed at room temperature.

2.5. Size-exclusion chromatography

Analytical size-exclusion chromatography was conducted using a G3000SWXL column (Tosoh, Japan). The mobile phase was a 20 mM sodium phosphate buffer solution (pH 7) containing 0.25 M NaCl. Flow rate was 0.5 mL/min. Sample volume was 20 μL and the sample concentration was 1 mg/mL.

2.6. Sodium dodecyl sulfate-polyacrylamide gel electrophoresis

Sodium dodecyl sulfate–polyacrylamide gel electrophoresis (SDS–PAGE) was conducted on 4–20% polyacrylamide gels commercially available from Daiich Pure Chemicals, Japan. Mab sample was loaded (5 μg/lane) gels were stained with silver for detection.

3. Model and calculation

3.1. Linear gradient elution model

We proposed and experimentally verified the method, by which the distribution coefficient K as a function of salt concentration I is determined from the protein peak salt concentration I_R in linear gradient elution. Below the method is explained briefly. The normalized gradient slope GH in linear gradient elution [3,6,8–10] is defined by the following equation:

$$GH = (gV_0)\left(\frac{V_t - V_0}{V_0}\right) = g(V_t - V_0) \quad (1)$$

where V_t is the total bed volume, V_0 the column void volume, $G = gV_0$ and $H = (V_t - V_0)/V_0$ is the phase ratio. g (M/mL) is the gradient slope of the salt, which is defined by the following equation:

$$g = \frac{I_F - I_0}{V_g} \quad (2)$$

where I_F is the final salt concentration, I_o the initial salt concentration, and V_g is the gradient volume. Linear gradient elution experiments are performed at different gradient slopes (GH values) at a fixed pH. The salt concentration at the peak position I_R is determined as a function of GH. The GH–I_R curves thus constructed do not depend on the flow velocity, the column dimension, the sample loading at non-overloading conditions, or the initial salt concentration I_o provided that the sample is initially strongly bound to the column [3,8]. The experimental GH–I_R data can usually be expressed by the following equation [3,8–10]:

$$GH = \frac{I_R^{(B+1)}}{[A(B+1)]} \quad (3)$$

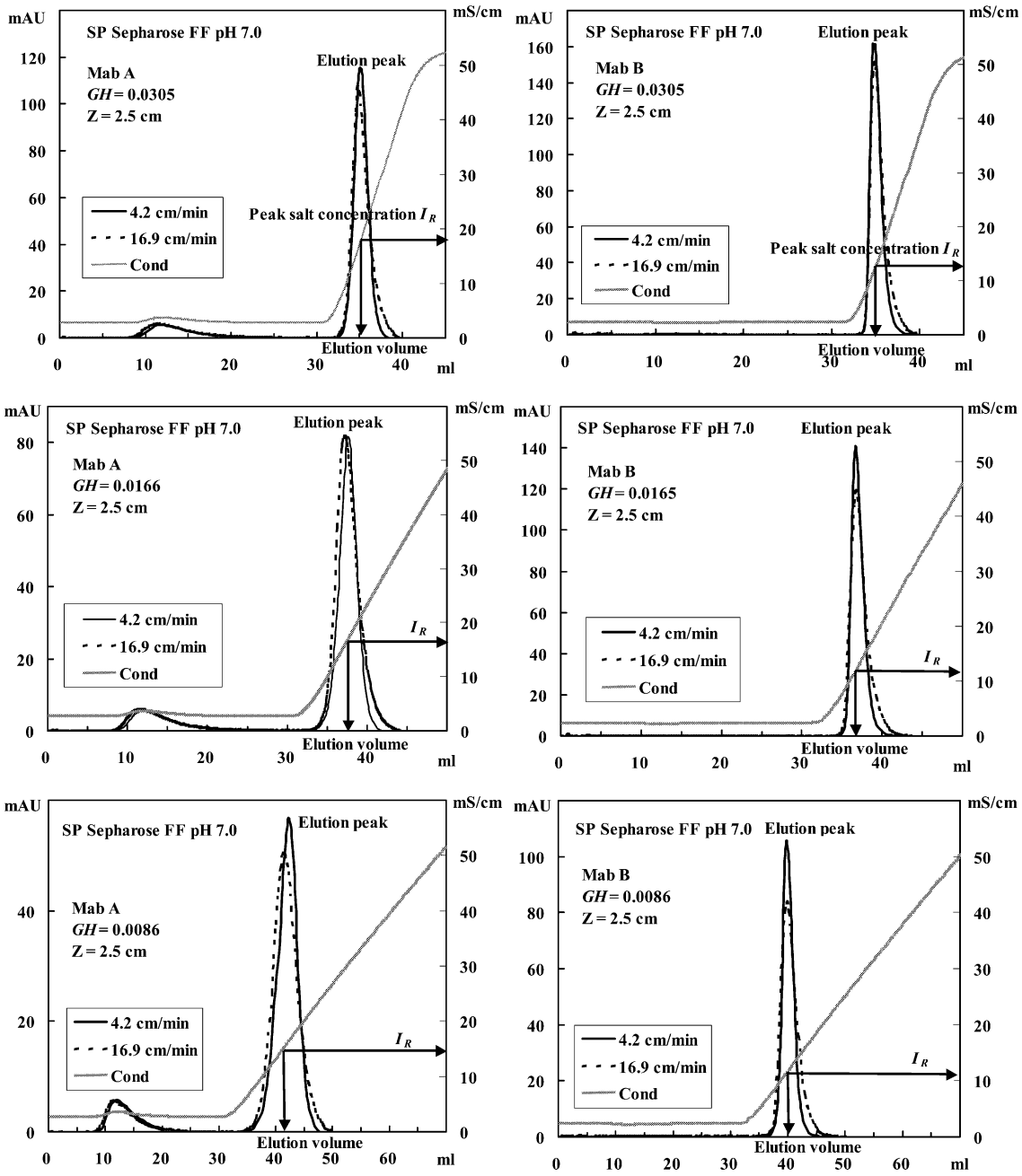

Fig. 1. Linear gradient elution curves of Mab A and Mab B as a function of flow velocity at different gradient slopes on cation-exchange chromatography.

From the law of mass action (ion-exchange equilibrium) [1–3,11–14], the following relationship can be derived:

$$A = K_e \Lambda^B \tag{4}$$

Here, B is the number of sites (charges) involved in protein adsorption, which is basically the same as the Z number [11] or the characteristic charge [14] in the literature, K_e is the equilibrium association constant, and Λ is the total ion-exchange capacity. From the ion-exchange equilibrium model [3,11–14] and Eq. (4), the following equation is derived [3]:

$$K - K' = K_e \Lambda^B I^{-B} \tag{5}$$

where K is the protein distribution coefficient, K' the distribution coefficient of salt, and I is the ionic strength (salt concentration).

Eq. (5) provides the K–I relationship, from which the stepwise elution condition (elution buffer salt concentration) can be determined [3].

The relative elution volume V_R/V_t of the stepwise elution is calculated by Eq. (6), as follows:

$$\frac{V_R}{V_t} = \varepsilon + (1-\varepsilon)K \tag{6}$$

From Eqs. (5) and (6), the relative elution volume as a function of ionic strength (salt concentration) and ion-exchange capacity can be obtained as useful information for process characterization [6].

3.2. Dimensionless parameter in linear gradient elution

In linear gradient elution of protein, the same resolution can be obtained with various combinations of gradient slope, column length, and flow rate based on the dimensionless variable O [8].

$$O = \frac{ZI_a}{\left[G(\mathrm{HETP})_{\mathrm{LEG}}\right]} \tag{7}$$

where Z is the column length, I_a a dimensional constant 1, G the gradient slope normalized with respect to column void volume, and $(\mathrm{HETP})_{\mathrm{LEG}}$ is the plate height in the linear gradient elution and calculated with the elution curves (retention time and peak width) from the linear gradient elution experiments [3,8].

4. Results and discussion

4.1. Gradient elution data analysis

Fig. 1 shows linear gradient elution curves of Mab A and Mab B as a function of flow velocity at different gradient slopes. As the flow velocity increases, the peak becomes wider while the peak position remains constant. When the gradient slope becomes steeper, the peak retention volume decreases whereas the peak salt concentration I_R increases. From these elution curves, the GH–I_R and the HETP–u relationships were determined. Fig. 2 shows the GH–I_R curves for Mab A and Mab B. The curves did not depend on the flow velocity, as mentioned in Section 3.1. This indicates the applicability of the model to the present experimental system. From the GH–I_R curves and Eq. (3), the values of A and B of Mab A and Mab B, respectively, were obtained as follows (Table 1).

Table 1
Parameters values obtained by gradient elution data analysis

	A	B
Mab A	5.97×10^{-7}	6.7
Mab B	3.45×10^{-10}	8.7

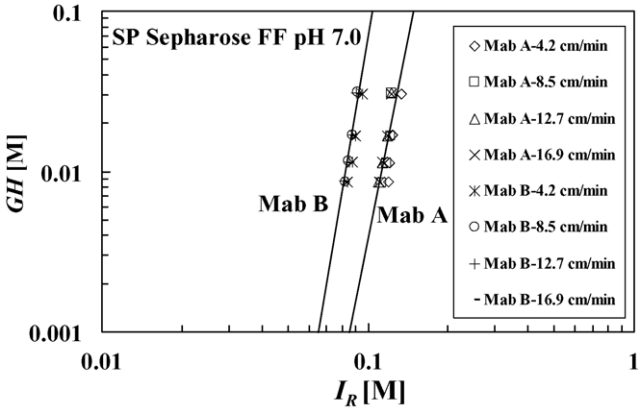

Fig. 2. GH–I_R curves for Mab A and Mab B on cation-exchange chromatography.

Fig. 3 shows the HETP–u plots of Mab A and Mab B. The experimental data can be expressed by a simplified Van Deemeter equation, $A^\circ + C^\circ u$, where A°, the intercept, is the contribution due to axial dispersion and the slope of the curve C° is the stationary phase diffusion resistance. The intercept values are very often quite large for the data at the binding conditions. It may be due to the fact that the contaminants are included in the main peak so that the peak width is an apparent value. Such apparent peak width also changes with the flow rate as the resolution may vary. We did not perform the detailed analysis on this curious and very frequently observed behavior as the purpose of this plot is just to show how the peak width changes with the flow rate and can be incorporated in the separation time-separation volume relationships.

4.2. Optimization of linear gradient elution

As a base-case, the following chromatography conditions were chosen for Mab A and Mab B (Table 2). The O values for these conditions are calculated as 144 (Mab A) and 166 (Mab B), respectively.

When the flow velocity u is increased, the gradient slope g must become shallower in order to obtain the same O value. Similarly, when u is decreased, g must be increased. With the aid of the HETP–u curve this calculation can be done. Once the u and the g values are determined, the separation time t_S and the buffer consumption BC are calculated as follows:

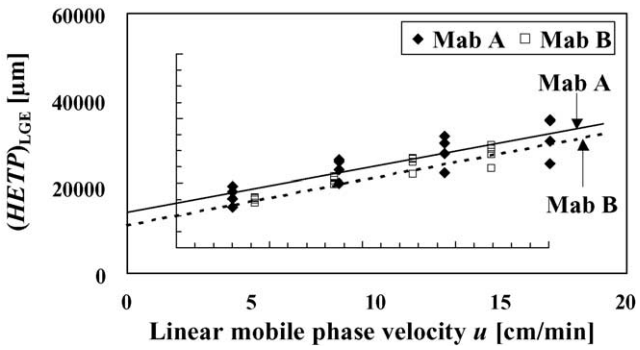

Fig. 3. $(\mathrm{HETP})_{\mathrm{LGE}}$ and u relationships on cation-exchange chromatography.

$$V_R = Ft_R = \left[(I_R - I_0)/g + V'\right]$$
$$I_R = I_0 + g\left(V_R - V'\right) \quad I_{inlet} = I_0 + gV$$
$$t_R = \left[(I_R - I_0)/g + V'\right]/F$$
$$t_R = \left[(I_R - I_0)/(gV_0) + \left(V'/V_0\right)\right](V_0/F)$$
$$t_R = \left[(I_R - I_0)/G + \left(1 + HK'\right)\right](Z/u) \quad (8)$$

here

$$V' = V_0(1 + HK')$$
$$V_R/V_t = Ft_R/V_t = Ft_R\varepsilon/V_t\varepsilon = Ft_R\varepsilon/V_0 = t_R\varepsilon/(Z/u) \quad (9)$$

We call the t_R–V_R/V_t curve at a constant O value the "iso-resolution curve" as the same resolution with different separation time and buffer consumption can be obtained on this curve.

In Fig. 4, the calculated iso-resolution curves are shown for Mab A and Mab B. The open circles are the data for the base case conditions. As shown in the figure, the separation time becomes longer as the elution volume decreases. On the contrary, large elution volume is needed for rapid separation. It is especially important to know where your separation conditions are located. For example, if your separation is carried out at point A in Fig. 4, it is not wise to decrease the flow velocity for reducing the buffer consumption. On the contrary, very large buffer consumption is needed in order to obtain a small reduction of separation time at point B in Fig. 4.

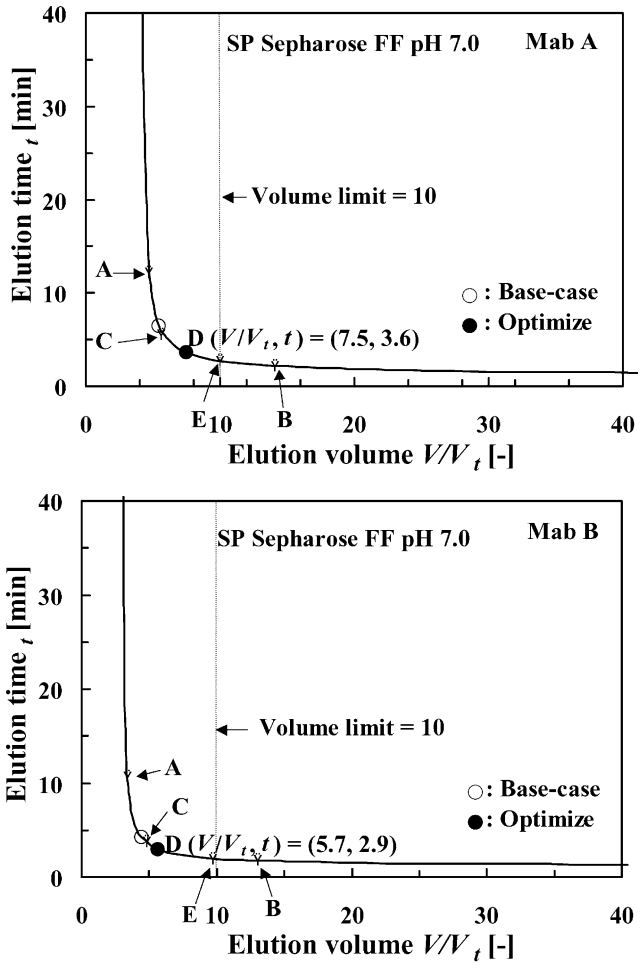

Fig. 4. Iso-resolution curves of Mab A and Mab B with cation-exchange chromatography.

Table 2
Base-case chromatography conditions

Flow rate (mL/min)	1.0
Gradient volume (column bed volume)	20
Column length (cm)	2.5

Table 3
Optimized chromatography conditions

	Flow rate (mL/min)	Gradient volume (column bed volume)	Column length (cm)
Mab A	2.0	28.9	2.5
Mab B	1.9	28.9	2.5

In this case, for optimization we tried to reduce the separation time than the base-case with the constraint of the elution volume less than 10 V_t. Optimized chromatography conditions were arbitrary points between point C and point E of the iso-resolution curves (Fig. 4). Point D was chosen as one of the optimized chromatography conditions (Table 3). It was not our purpose to perform mathematically rigorous optimization procedures.

The predicted values for separation time and elution volume for point D are shown in the figures, which are in good agreement with the experimental values (see Figs. 4 and 6).

Using the iso-resolution curve we can examine the impact of column length on separation time-elution volume relationship [15].

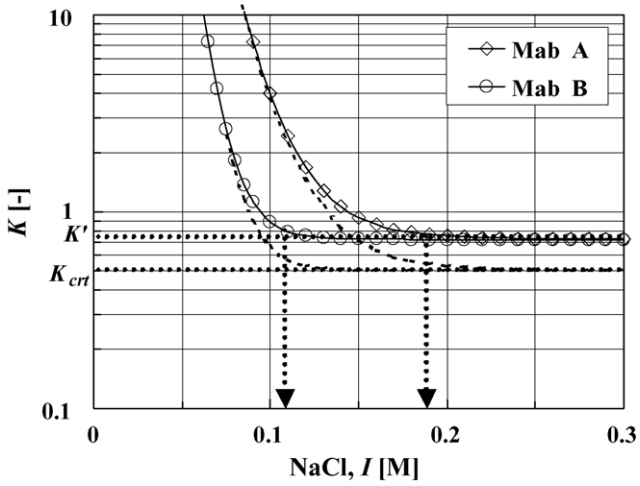

Fig. 5. Relationship between distrubution coefficient K and salt (NaCl) concentration I. K' is the K value of the salt and K_{crt} is the K value at non-binding conditions (size-exclusion mode). Note that K_{crt} is less than K' for porous bead.

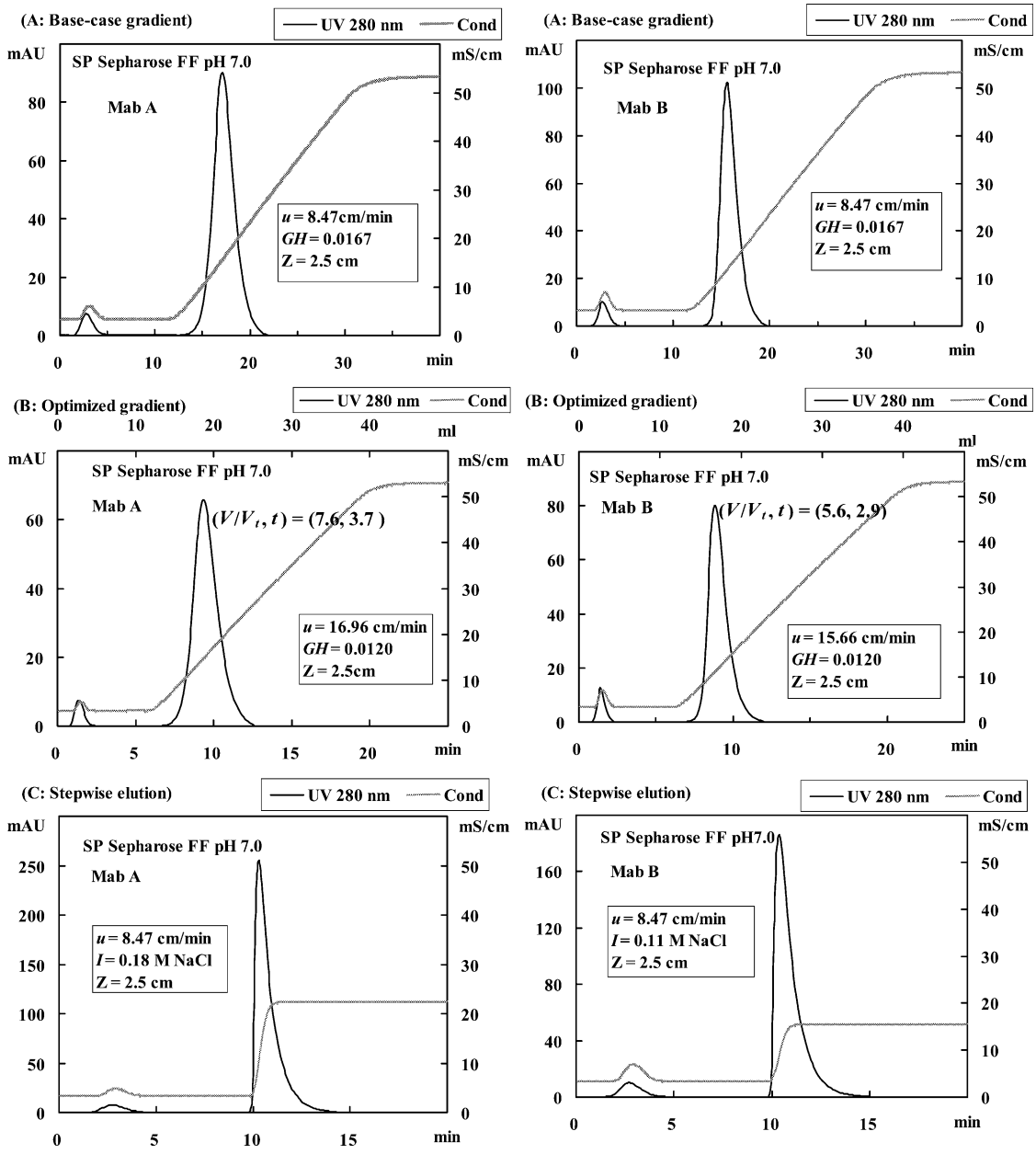

Fig. 6. Elution curves of Mab A and Mab B with cation-exchange chromatography column. The *O* values in (A) and (B) were set equal. Note that because HETP is not proportional to *u* (*uGH*), the values are not equal in (A) and (B). Salt concentration of stepwise elution (C) was determined from *K–I* curves (derived from GH–I_R curves). Column: SP Sepharose FF (2.5 cm × 0.7 cm i.d.), sample: 1 mL Mab A or Mab B (1 mg/mL) solution.

4.3. Optimization of stepwise elution

Fig. 5 shows the *K–I* curves derived from the *A* and *B* values. Stepwise elution can be divided into two types. In type I elution, a sharp peak is eluted in the front end of the elution buffer because of the peak sharpening effect [3]. In type II elution the peak appears after the column is saturated with the elution buffer. In this case the peak width and the peak retention time are similar to those in isocratic elution with the same elution buffer [3]. It is therefore advantageous to employ type I stepwise elution. However, when the elution buffer salt concentration I_E is too high, impurities strongly bound to the column as well as the target protein may be eluted simultaneously. This may result in lower purity than gradient elution. Type I elution is accomplished when the protein distribution coefficient at I_E is less than the distribution coefficient of salt K'. From Fig. 5, the I_E values for type I elution were determined as 0.18 M NaCl (Mab A) and 0.11 M NaCl (Mab B). At these I_E values the corresponding K values are lower than K' (= 0.72).

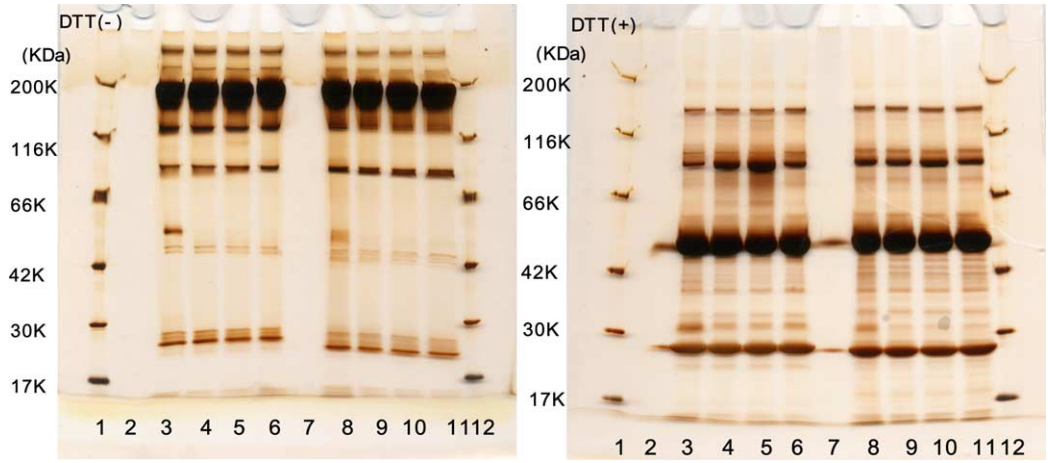

Fig. 7. SDS–PAGE (silver staining) from SP Sepharose FF chromatography. Lanes: (1 and 12) molecular mass standards; (3) Mab A SP FF load; (4) Mab A SP FF pool base-case gradient; (5) Mab A SP FF pool optimized gradient; (6) Mab A SP FF pool stepwise elution; (8) Mab B SP FF load; (9) Mab B SP FF pool base-case gradient; (10) Mab B SP FF pool optimized gradient; (11) Mab B SP FF pool stepwise elution. *Note*: 5 μg/lane except molecular mass standard. kDa, kilo Dalton and K = ×1000.

Table 4
The recovery ratio and the purity values determined by size-exclusion HPLC (HPSEC)

	Mab A		Mab B	
	Recovery (%)	Purity (%)	Recovery (%)	Purity (%)
Base-case gradient	92.1	98.7	88.2	99.1
Optimized gradient	94.3	98.8	93.4	98.9
Stepwise elution	85.0	98.8	88.0	99.0

Note: Purity of load samples of Mab A and Mab B were 98.2% and 97.8%, respectively. Peak collection criteria were as follows: elution was fractionated as 1 mL/fraction. The fractions in the range of the UV output that is over 3% of the peak height were collected as the pooled fraction.

4.4. Evaluation of optimized condition

To verify the optimized chromatography conditions determined above, the elution curves, the recovery and the purity were evaluated.

Fig. 6 shows the elution curves of Mab A and Mab B on SP Sepharose FF by base-case gradient, optimized gradient and stepwise elution chromatography conditions. The elution time of the optimized gradient elution was shortened compared with those of the base-case condition, as expected. The predicted values for separation time and elution volume for point D are shown in the figures, which are in good agreement with the experimental values (see Figs. 4 and 6).

Typical type I elution curves were obtained for stepwise elution. The elution curves are sharp without peak tailing or leading. These results indicate that the present method is useful to determine the stepwise elution conditions from the linear gradient elution data.

The recovery ratio and the purity values determined by size-exclusion HPLC (HPSEC) are summarized in Table 4. Both the recovery ratio and the purity values are quite high in all chromatography results. As shown in Fig. 7 the SDS–PAGE data also showed high purity of the recovered fraction from these chromatography runs. Generally, in the case of silver stained SDS–PAGE analysis of Mab, several bands like Fig. 7 can be observed, although the purity of the Mab is high (please refer to Table 4, HPSEC purity is ca. 99%). This is because of the degradation of the Mab during the pretreatment of SDS.

These results indicate that the optimized chromatography conditions were acceptable in terms of the purity and the recovery as well as the reduced process time.

Type II stepwise elution is sometimes unstable because a small change in pH, salt concentration and ion-exchange capacity affects the elution volume significantly [6]. However, type I elution is less sensitive to such parameters although the condition that K at I_E is less than K' must be fulfilled.

5. Conclusion

Monoclonal antibody purification processes by cation-exchange chromatography were first analyzed by our simple method that uses linear gradient elution experimental data. By using the iso-resolution curve concept, the optimized conditions were determined for linear gradient elution. Efficient stepwise elution (type I elution) conditions were determined from the distribution coefficient as a function of salt concentration. The optimized linear gradient and stepwise elution were successfully carried out in terms of the peak shape, the recovery and the purity value.

References

[1] G. Sofer, L. Hagel, Handbook of Process Chromatography, Academic Press, San Diego, CA, 1997.

[2] E. Karlsson, L. Ryden, J. Brewer, in: J.-C. Janson, L. Ryden (Eds.), Protein Purification, second ed., Wiley-VCH, New York, 1998, pp. 145–205.
[3] S. Yamamoto, K. Nakanishi, R. Matsuno, Ion-Exchange Chromatography of Proteins, Marcel Dekker, New York, 1988.
[4] M. Ladisch, Bioseparations Engineering: Principles, Practice, and Economics, Wiley, New York, 2001.
[5] P. Gagnon, Purification Tools for Monoclonal Antibodies, Validated Biosystems, 1996.
[6] S. Yamamoto, P. Watler, D. Feng, O. Kaltenbrunner, J. Chromatogr. A 852 (1999) 37.
[7] G. Guiochon, S. Shirazi, A. Katti, Fundamentals of Preparative and Nonlinear Chromatography, Academic Press, New York, 1994.
[8] S. Yamamoto, Biotechnol. Bioeng. 48 (1995) 444.
[9] S. Yamamoto, T. Ishihara, J. Chromatogr. A 852 (1999) 31.
[10] S. Yamamoto, T. Ishihara, Sep. Sci. Technol. 35 (2000) 1707.
[11] W. Kopaciewicz, M.A. Rounds, J. Fausnaugh, F.E. Reniger, J. Chromatogr. 266 (1983) 3.
[12] N.K. Boardman, S.M. Partrige, Biochem. J. 59 (1955) 543.
[13] C.M. Roth, K.K. Uger, A.M. Lenhoff, J. Chromatogr. A 726 (1996) 45.
[14] S.R. Gallant, S. Vunnum, S.M. Cramer, J. Chromatogr. A 725 (1996) 295.
[15] S. Yamamoto, J. Chromatogr. A, submitted for publication.